

THE PENNSYLVANIA STATE UNIVERSITY
SCHREYER HONORS COLLEGE

DEPARTMENT OF MATERIALS SCIENCE AND ENGINEERING

Reversible Actuation and Property Recovery of Amphiphilic Triblock Copolymer Fibers
Produced by Wet-Spinning

KELLY MATUSZEWSKI
SPRING 2022

A thesis
submitted in partial fulfillment
of the requirements
for a baccalaureate degree
in Materials Science and Engineering
with honors in Materials Science and Engineering

Reviewed and approved* by the following:

Robert Hickey
Assistant Professor of Materials Science and Engineering
Thesis Supervisor

Allen Kimel
Associate Teaching Professor of Materials Science and Engineering
Honors Adviser

* Electronic approvals are on file.

ABSTRACT

The development of small-scale actuators for applications in soft robotics and artificial muscles is a growing field in the space of materials science research. Polymeric materials have potential in the space of soft actuators because of their ability to provide small-scale stimuli responsiveness, compliance, and light weight. The work presented in this thesis explores how the triblock copolymer system of polystyrene-*b*-poly(ethylene oxide)-*b*-polystyrene (SOS) can be utilized as a small scale fiber actuator which is responsive to heat and moisture stimuli. The creation of fiber actuators is a two-step process in which physically crosslinked hydrogel fibers are first made and then strained to form highly aligned PEO crystalline domains. Triblock copolymer self-assembly and the formation of physical crosslinks provides mechanical stability to the hydrogel. Gel fibers are produced using wet-spinning, which utilizes solvent-non-solvent rapid injection of dissolved polymer solution into water. Wet-spinning introduces uniform processing and controlled injection rate compared to previous methods of hand injection. Once hydrogel fibers were made, they were strained to 5x their original length to induce crystallization of the poly(ethylene oxide) block along the length of the fiber. These crystals can be melted at temperatures above 66 °C or when exposed to water, producing an actuation response. In this work, the actuation behavior in response to these stimuli and the subsequent actuation properties were measured. Results in this study demonstrate that the actuation length change, actuation velocity, and energy density are reversible processes. The properties are fully recoverable for at least two cycles once the fiber has been restrained. This study also investigates the dependence of actuation properties on needle gauge, strain rate, and actuation stimulus. This thesis aims to establish a fundamental understanding regarding the use of triblock copolymer fibers as actuators in the growing field of soft robotics.

TABLE OF CONTENTS

LIST OF FIGURES	iii
LIST OF TABLES	iv
ACKNOWLEDGEMENTS	v
Chapter 1 Introduction	1
1.1 Technical Motivation	1
1.2 Polymer Fiber Production Methods	4
1.3 Copolymer Self-Assembly and Actuation.....	5
Chapter 2 Wet-Spinning Implementation	9
2.1 Polymer Preparation.....	9
2.2 Wet-Spinning	10
2.3 Physical Property Analysis	12
Chapter 3 Fiber Actuation Characterization Methods	17
3.1 Actuation Stroke.....	17
3.2 Actuation Velocity	18
3.3 Energy/Work Density.....	19
Chapter 4 Fiber Actuation Results and Discussion.....	21
4.1 Actuation Stroke.....	21
4.2 Actuation Velocity	22
4.3 Energy/Work Density.....	23
Chapter 5 Conclusion and Future Work	26
BIBLIOGRAPHY.....	28

LIST OF FIGURES

Figure 1: Progression images of polymer fiber exhibiting linear actuation triggered by heat [6]	2
Figure 2: Diagram of wet-spinning polymer fiber production method [9]	4
Figure 3: Diagram of amphiphilic ABA triblock copolymer self-assembly and the effects of increased polymer concentration [8]	6
Figure 4: Diagram of SOS triblock copolymer and how the polymer self-assembles in water	7
Figure 5: (a-d) 2D WAXS scattering results with respect to fiber strain, and (e) diagram of hypothesized domain structure of the SOS fibers [10]	8
Figure 6: Diagram of wet-spinning apparatus used in creation of hydrogel fibers	11
Figure 7: Optical microscopy images of (a) wet-spun hydrogel fiber and (b) a 5x strained and dried polymer fiber	13
Figure 8: (a) Picture of hydrogel fibers created through non-equilibrium processing and (b) an SEM image of a freeze-dried hydrogel fiber under SEM imaging [10]	14
Figure 9: Stress versus strain plot for SOS CE7 swollen hydrogel fiber	15
Figure 10: Load versus time plot for mechanical analysis of crystallization force	16
Figure 11: Diagram of method used to measure reversibility of properties	18
Figure 12: Example of actuation length change seen when fibers are exposed to water or heat [10]	20
Figure 13: Plots of calculated actuation stroke values versus (a) change in initial strain rate and (b) number of times the fiber has been actuated	21
Figure 14: Plot of linear actuation speed versus the number of times the fiber has been actuated, and (b) picture of method of actuating fiber with water	22
Figure 15: Plot of rotational actuation achieved for pre-rotated hydrogel fiber actuated with water	23
Figure 16: Energy density versus (a) cycle, (b) actuation trigger, and needle gauge	24

LIST OF TABLES

Table 1: Molecular weight, dispersity, and coupling efficiency data for SOS copolymer samples	9
Table 2: Needle gauges and inner diameter of syringes used for wet-spinning.....	12
Table 3: Diameter and standard deviation values for 5x strained dried fibers made with varying needle gauges	13

ACKNOWLEDGEMENTS

Special thanks to Dr. Robert Hickey for supporting this research project and for his mentorship throughout my four years of undergraduate research experience. I would also like to acknowledge Dr. Chao Lang and Elisabeth Lloyd for their help and support, as well as for the preparation and characterization of the triblock copolymers used in this project. This project would not be possible without their hard work and dedication to this exciting research. I would like to also thank and acknowledge the NSF DMREF program (CMMI 2119717) and Penn State MRI Seed Grant for funding this research. Any opinions, findings, and conclusions or recommendations expressed in this publication are those of the author and do not necessarily reflect the views of the NSF.

I would also like to thank the Penn State MatSE Department for their support over these past four years. I am incredibly thankful for my time in this department and for what I have learned through my time here. The MatSE community has always been incredibly supportive, and I am thankful for the friendships I have created. Finally, I would like to thank my family as none of this would be possible without your incredible love and support.

Chapter 1

Introduction

1.1 Technical Motivation

The field of robotics and wearable electronics has revolutionized industry and manufacturing, and recent advances in materials science has contributed to increased complexities in design [1]. Some of these complexities include small scale adaptability, stimuli response, and improved interfaces with the human body [1,2,3]. These improvements, made possible by the use of soft materials, have led to the development of the field of soft robotics. Soft robotics often utilizes polymers because of their light weight, flexibility, compliance, and potential for response to external stimuli [4,5]. Particularly, the potential for dynamic polymer fibers to replicate biological muscle structure and actuation mechanisms is an active area of research because this has not yet been achieved synthetically [3,6]. Some polymers have the ability to introduce of dynamic stimuli responses and enhanced small-scale functionality as soft actuators, which provides opportunities in biological and industrial applications [3]. Soft actuators have the potential to be used in medical applications as artificial muscles and wearable sensors [4,5]. There is also potential for the fibers to be woven into textile actuators for use in wearable artificial muscles or other assistive biomedical devices [7]. Furthermore, recent advances in polymer-based actuators have enabled utilization as soft grippers, sensor-integrated soft robotics, and haptic displays [3]. An example of a polymer fiber exhibiting linear actuation as it performs as an artificial muscle is shown in Figure 1.

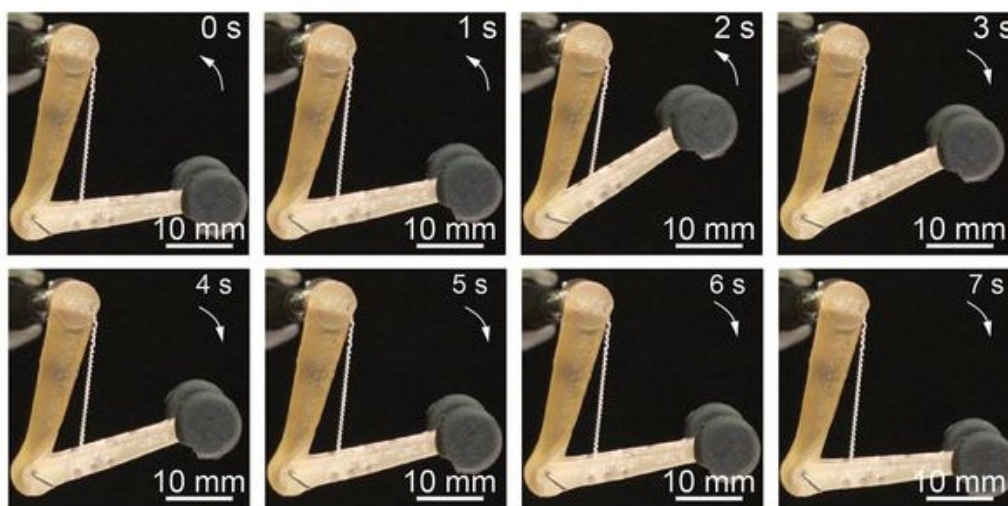


Figure 1: Progression images of polymer fiber exhibiting linear actuation triggered by heat [6]

This project investigates the potential for polystyrene-*b*-poly(ethylene oxide)-*b*-polystyrene (SOS) triblock copolymer fibers to be used as soft actuators for applications in soft robotics and artificial muscles. The amphiphilic ABA triblock copolymer system discussed here has potential as a dynamic actuator because reversible linear and rotational actuation is achieved by exposing the poly(ethylene oxide) (PEO) crystals to heat or water. Previous work by Lang et al. has outlined non-equilibrium processing of SOS hydrogel fibers, and the work in this thesis builds on that knowledge [8]. For the procedure in this project, the hydrogel fibers are first produced through non-equilibrium wet-spinning processing, strained while swollen with water, dried, and actuated. Equilibrium processing would be achieved by slow evaporation of the solvent or hydrating the block copolymer over time, while non-equilibrium hydrogel production involves injecting a dissolved solution of SOS into water which is a non-solvent for polystyrene (PS) [8]. Non-equilibrium processing is beneficial because rapid diffusion of solvent out of the structure creates large pores which fill with water and leads to a very high swelling ratio furthered described in Chapter 2.3.

Also, Lang et al. studied the effects of SOS self-assembly in a non-solvent such as water [8]. On contact with water, the PS blocks self-assemble into micelles to minimize their interaction with water, and these micelles are bridged together by hydrophilic PEO chains. Hydrogel fibers made via non-equilibrium processing depend on self-assembly and physical crosslinking from micellization for their mechanical stability. The PEO block, which will crystallize when dry, ultimately leads to the actuation properties which enable this fiber to potentially be used in soft robotics applications as a linear or rotary actuator. Analysis into fiber production and self-assembly is further discussed in Chapters 1.2 and 1.3 respectively.

It is necessary to consider certain actuator performance indicators to compare the SOS polymer system to current soft actuators and biological tissues. Characterizing actuator performance involves measuring values for the actuation stroke, actuation force, energy density, and reversibility [3]. The actuation stroke describes the change in length which occurs upon actuation and actuation force is the force measured when the actuator is triggered by a certain stimulus. In literature, soft actuators have been responsive to electrical, magnetic, chemical, thermal, light, and pressure driven stimuli [2]. When comparing actuator performance, it is also important to consider the applications they will be used in. For example, some considerations include size scale, biocompatibility, operating environment, fatigue resistance, and response time [2]. In the following analysis, data is included for swelling ratio, mechanical properties, actuation stroke, actuation speed, cycle life, fiber diameter, and energy density. These values will be compared to the properties of other soft actuators and muscle fibers because the field of soft robotics strives to replicate the performance of biological tissue [3].

1.2 Polymer Fiber Production Methods

As previously mentioned, linear and rotational actuation of the SOS triblock copolymer system is achieved through the creation of polymer fibers with aligned semicrystalline regions in which the PEO chains are aligned in the direction of the fiber length. In industry, the creation of large quantities of polymer fiber is made possible through four main methods of polymer fiber spinning [9]. The four main methods of polymer fiber spinning include electrospinning, melt spinning, dry spinning, and wet spinning. To continue with solvent-non-solvent non-equilibrium processing from Lang et al., wet-spinning was selected as the processing method of choice for more uniform production of fibers. Wet spinning involves the injection of the dissolved fiber solution into a coagulation bath and subsequent removal using a spinning rod, as depicted in Figure 2. Wet spinning has been used extensively for the production of fibers used in biomedical applications such as scaffolding for cartilage and tissue repair [9]. Through the use of controllable polymer spinning methods, it is easy to adjust flexibility, material choice, and mechanical properties.

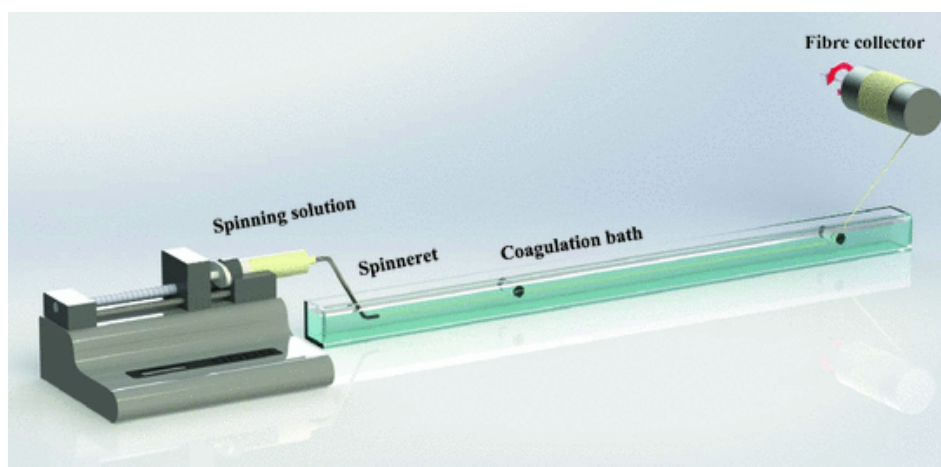


Figure 2: Diagram of wet-spinning polymer fiber production method [9]

As previously mentioned, wet spinning is necessary to continue non-equilibrium processing and promote self-assembly during rapid solvent exchange. Previously, the polymer solution was rapidly injected into the water bath by hand which enabled inevitable human error in fiber processing. Wet-spinning introduces control over more processing parameters such as injection speed, coagulation bath stir bar speed, nozzle diameter, and polymer concentration. Now, with the use of an injection pump, it is possible to work towards establishing processing/structure/property relationships. The specific wet spinning methodology used can be found in Chapter 2.2.

1.3 Copolymer Self-Assembly and Actuation

Currently studied polymeric soft-actuators utilize liquid-crystal polymers, networks, and elastomers or shape-memory polymers [2]. A novel system for actuation which requires further research is block copolymers. The polymer system for this project is an ABA amphiphilic triblock copolymer. The PS A blocks are hydrophobic, and the PEO B block is hydrophilic. Amphiphilic copolymers have been widely used in medical applications such as tissue engineering due to their self-assembly and subsequent drug carrying capacity [9]. Self-assembly occurs when the polymer is in a B-selective solvent such as water, and this is important in the field of soft robotics because it is crucial for actuation [8].

During self-assembly in water, the hydrophobic PS A blocks will form aggregates which physically crosslink through bridges formed by the hydrophilic PEO B block [8]. The polymers will only form hydrogels in water if the polymer concentration in a good solvent is above the critical overlap concentration, c^* . This c^* factor is used to describe when polymer chains begin

to overlap in solution, which is critical for bridging the aggregates together to form physical crosslinks. If the chains are not entangled, then they will only self-assemble to form microgels or micelles which have a higher degree of looping than bridging between the chains, as seen in Figure 3. Once the polymer is dissolved within the entanglement regime in a good solvent, it can then be injected into water which is a poor solvent for the A block and leads to aggregation.

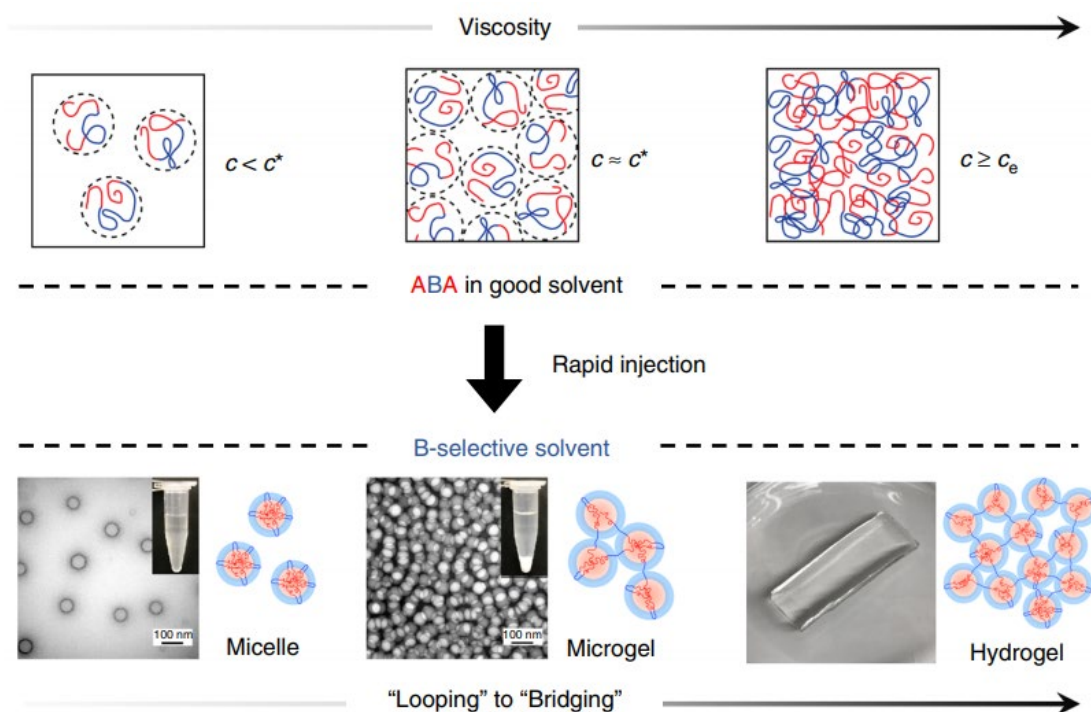


Figure 3: Diagram of amphiphilic ABA triblock copolymer self-assembly and the effects of increased polymer concentration [8]

The capability of the SOS triblock copolymer fiber to actuate is enabled through the aforementioned self-assembly of the amphiphilic blocks when injected into water. It is also important that the PEO block is a semicrystalline and hydrophilic block, while oppositely there is a hydrophobic amorphous region formed by the PS blocks. When SOS is injected into water via the wet-spinning process, the hydrophobic PS blocks aggregate to form cores which are bridged together by the hydrophilic PEO blocks seen in Figure 4. The PEO blocks between the PS cores

serve as physical crosslinks to give the hydrogel fiber its mechanical strength. Aggregation and bridging are important for the mechanical properties and future crystallization of the fibers when strained. As stated previously, non-equilibrium processing is beneficial because rapid diffusion of the solvent out and water into the structure creates large pores which leads to a very high swelling ratio.

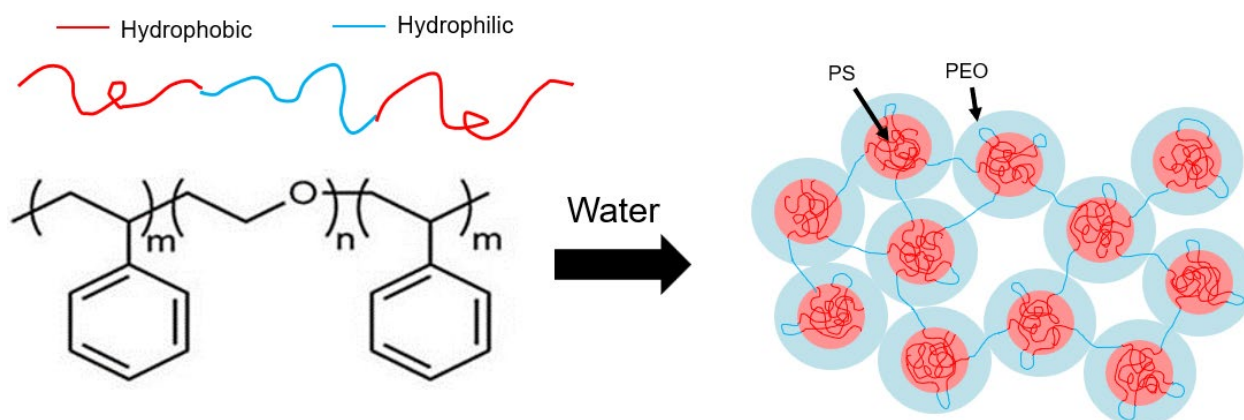


Figure 4: Diagram of SOS triblock copolymer and how the polymer self-assembles in water

To enable linear actuation, the fibers are strained while swollen with water which allows the PEO blocks to align and crystallize. The crystallization which occurs has been recently characterized by Lang et al. through x-ray scattering results which show increased crystal alignment with an increase in initial strain of the swollen fibers [10]. Data for wide angle x-ray scattering (WAXS) is shown in Figures 5(a-d). As the fiber is strained to longer lengths, the WAXS pattern shows that the crystalline domains are aligning in the same direction as opposed to being randomly configured as shown in Figure 5(a).

Crystallization and alignment of PEO domains, demonstrated by Figure 5(e), sets up the mechanism for actuation triggered by water and heat because these stimuli melt the PEO crystals. When the PEO crystals are melted, they lose their shape and alignment, and this allows the PS cores to expand and the fiber to contract. In Figure 5(e), the blue chains are the PEO

crystalline domains, and the red chains are the amorphous PS domains, and this forms an ordered structure of crystalline and amorphous domains. The actuation properties of the fibers were studied in detail to understand the physical and mechanical properties which arise from the unique microstructure of the triblock copolymer system and non-equilibrium production method.

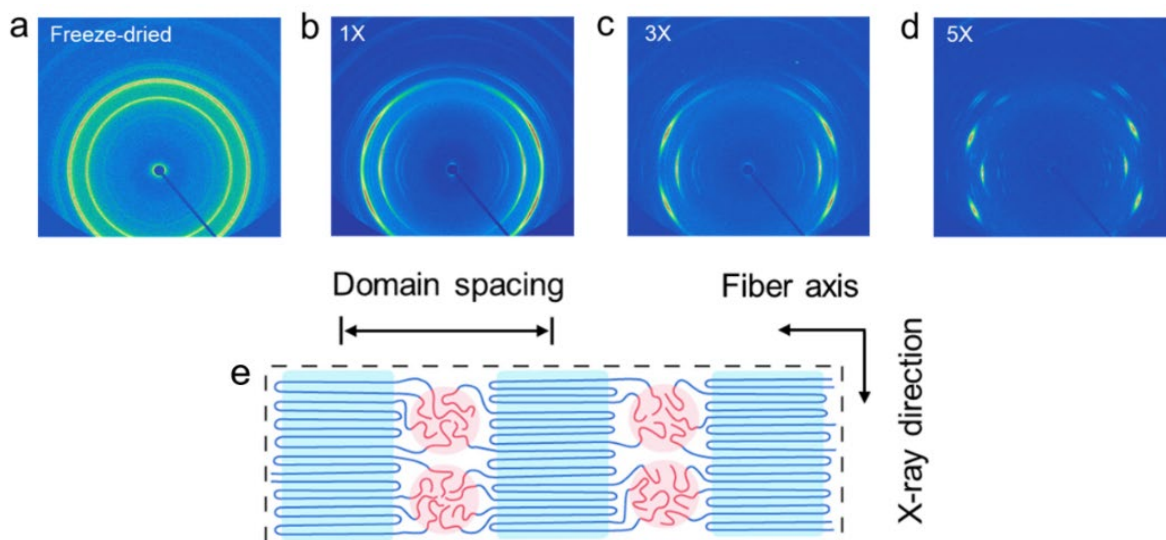


Figure 5: (a-d) 2D WAXS scattering results with respect to fiber strain, and (e) diagram of hypothesized domain structure of the SOS fibers [10]

Chapter 2

Wet-Spinning Implementation

2.1 Polymer Preparation

The SOS triblock copolymer samples were prepared via sequential living anionic polymerization of a PS-PEO diblock followed by a coupling reaction which joined the PEO blocks and created a triblock. Anionic polymerization helps to reduce the dispersity of the polymer, and a narrow molecular weight distribution affords more control over the self-assembly process [10]. The properties of the two SOS polymer samples used are located in Table 1. The second column in Table 1 describes the molecular weight of the PS end blocks and PEO midblock in the order of PS-PEO-PS. Molecular weight and dispersity were characterized by size-exclusion chromatography (SEC) on a Wyatt THF SEC equipped with a multi-angle light scattering detector. Coupling efficiency is a measure of how many diblock copolymers polymerized into triblock copolymers during the final coupling step and was characterized based on the calculated diblock molecular weight. Two different polymers were used for the research, and each research parameter was evaluated with separate sets of samples to limit variability. Future research will explore the effect of the PEO mid-block molecular weight on actuation properties.

Table 1: Molecular weight, dispersity, and coupling efficiency data for SOS copolymer samples

Name	Polymer	Mn (kg/mol)	Dispersity	Coupling Efficiency
CE3	SOS(13-74-13)	77.3	1.067	54%
CE7	SOS(13-153-13)	121.5	1.106	35%

To prepare the sample for wet-spinning, the polymer was dissolved in a solvent which dissolves both the PS and PEO blocks and is miscible with water. Tetrahydrofuran (THF) was used as the solvent for this process. First, the copolymer was cut into small pieces to aid in the dissolving process and weighed into a glass vial. Then, THF was added to the vial via a micropipette. The volume of THF added was dependent on the desired weight percent and calculated by Equation 2.1 where m_p is the polymer mass, c is the weight fraction, and ρ_s is the solvent density. The weight fraction is important because as seen previously in Figure 3, the polymer concentration must be large enough to allow for bridging of the micelles during self-assembly. The weight percent of each hydrogel fiber sample ranged from 12-22% and exact values will be noted for each result.

$$V_s = \frac{\frac{m_p}{c} - m_p}{\rho_s} \quad (2.1)$$

2.2 Wet-Spinning

Hydrogel fibers were produced by wet-spinning which utilizes non-equilibrium processing but incorporates a constant injection speed rather than nonuniform injection by hand. For the wet-spinning process, the polymer solution prepared from the procedure outlined in Chapter 2.1 was taken up into a syringe and the syringe was secured to an injection pump. Then, a 90° bent needle was attached to the syringe for subsequent injection of the solution into the coagulation bath. Figure 6 shows a diagram of the specific wet-spinning set-up used for this project. The coagulation bath was placed on a stir plate and was filled with reverse osmosis (RO) water and contained a stir bar. The stir bar was necessary because THF is less dense than water,

so as the THF diffused out of the fibers upon injection, the fibers would float to the top and lose their shape. The vortex created by the stir bar ensured the fibers were pulled inwards as opposed to upwards towards the surface.

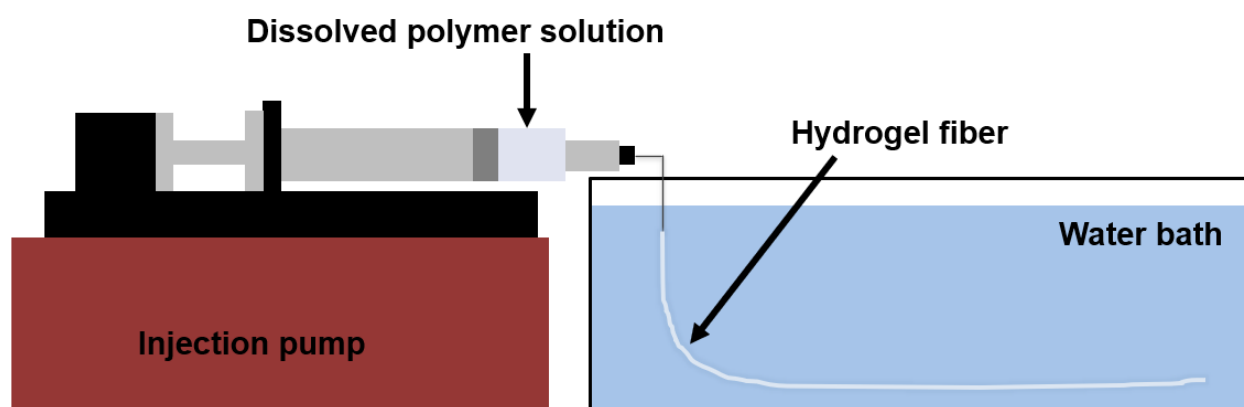


Figure 6: Diagram of wet-spinning apparatus used in creation of hydrogel fibers

Next, an injection speed was selected on the injection pump to begin the wet-spinning process. The injection speed used for process was 2.0 mL/min for the 19 gauge needle and 2.5 mL/min for the 22 gauge needle. Further studies are needed to determine the relationship between injection speed and the physical properties of the hydrogel fibers. The inner diameter for each needle is shown in Table 2, and the inner diameter of the 22 gauge needle is about 3/5 the size of the diameter of the 19 gauge needle. The syringe needle gauge was varied to measure the effects of fiber diameter on actuation properties. The needle gauge and inner needle diameter values used for actuation measurements are found in Table 2. Once a variety of fibers were formed by wet-spinning, they were placed into vials of RO water and stored in a fridge to prevent potential changes to the microstructure of the fiber over time.

Table 2: Needle gauges and inner diameter of syringes used for wet-spinning

Needle Gauge	Inner Diameter (μm)	Injection Speed (mL/min)
19	813	2.0
22	482	2.5

2.3 Physical Property Analysis

To have a better understanding of SOS hydrogel fibers prepared by wet-spinning, analysis was performed on the physical properties of diameter, swelling ratio, mechanical properties, and force generated during crystallization of the fiber held at a constant length. The diameters of swollen hydrogel fibers and 5x strained fibers were analyzed via optical microscopy using the Zeiss Axiovert 200 inverted optical microscope. The values calculated by this analysis method were used in the calculations of energy density since the diameter enables calculation of fiber volume. Example images of an SOS CE7 swollen hydrogel fiber direct from wet-spinning and a 5x strained and dried SOS CE7 fiber are seen in Figure 7(a) and 7(b) respectively.

As previously mentioned, during the wet-spinning process, different needle diameters were used to evaluate the fiber diameter's effect on properties. The difference in fiber diameter between the different gauges used are listed in Table 3. The standard deviation for the diameter values found is also provided in the table to compare fiber uniformity. The difference in needle gauge diameter between 22 and 19 gauge around 3/5 but the difference in fiber diameter once they are strained 5x their original length is close to a ratio of 3/4.

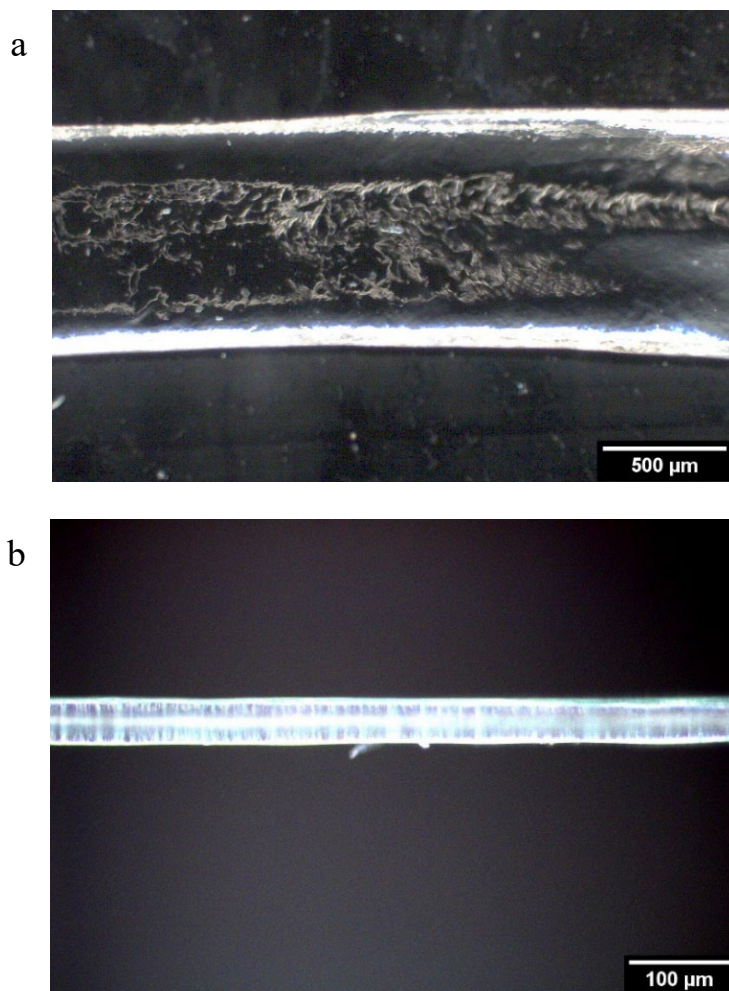


Figure 7: Optical microscopy images of (a) wet-spun hydrogel fiber and (b) a 5x strained and dried polymer fiber

Table 3: Diameter and standard deviation values for 5x strained dried fibers made with varying needle gauges

Needle Gauge	Fiber Diameter (μm)	Standard Deviation (μm)
19	102.7	12.2
22	77.2	11.6

The SOS CE7 hydrogel fibers were analyzed to calculate the swelling percent of water in the polymer by weight. This was done by first taking swollen hydrogel fibers, seen in Figure 8(a), and measuring their initial weight. Then, after three days of air drying in a fume hood, the samples were weighed again to measure the final mass of the dried polymer. The resulting swelling percent, calculated with Equation 2.2, was calculated to be 97.5% water by weight. This large swelling ratio is hypothesized to be caused by the large pores left by rapid solvent transfer between THF leaving the system and water entering. The pores can be seen in the SEM image from Lang et al. of a freeze-dried hydrogel fiber shown in Figure 8(b).

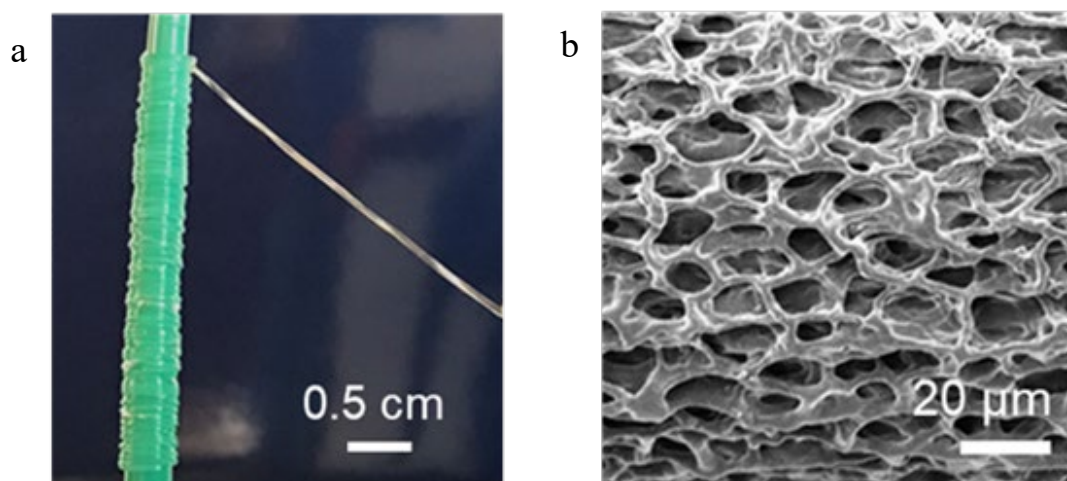


Figure 8: (a) Picture of hydrogel fibers created through non-equilibrium processing and (b) an SEM image of a freeze-dried hydrogel fiber under SEM imaging [10]

$$Swelling \% = \frac{(mass\ swollen - mass\ dried)}{mass\ swollen} * 100\% \quad (2.2)$$

Mechanical analysis was also performed on the as prepared hydrogel fibers to measure the mechanical properties, force generated by crystallization of the PEO measured at a constant length, and time associated with the crystallization process. For this analysis, an MTS Criterion load frame was used with a 10 N load cell. A stress strain curve for an SOS CE7 hydrogel fiber

dissolved at 20 weight percent in THF is shown in Figure 9 with a moving average of 15 periods. The Young's modulus was calculated to be 3.55 kPa. This value is comparable to muscle fibers which have Young's modulus values ranging from 7.4 to 14.6 kPa depending on the type of muscle and its use [11].

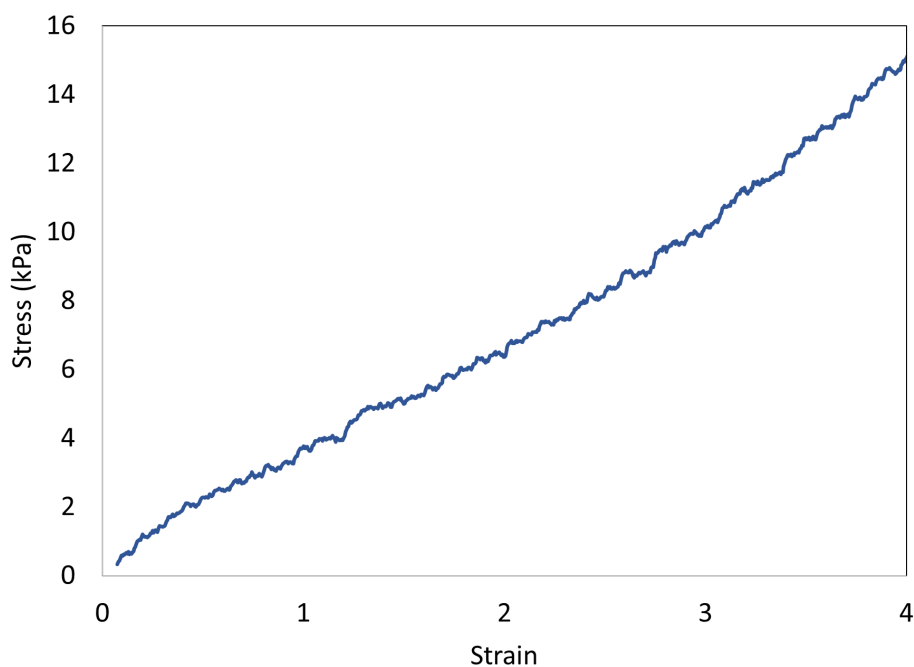


Figure 9: Stress versus strain plot for SOS CE7 swollen hydrogel fiber

Along with mechanical analysis, the load frame was utilized to measure the force generated during crystallization when the fiber was held at a constant length. When a polymer crystallizes, it becomes more dense than the amorphous phase because of alignment of the chains in a certain orientation which allows for tight chain packing. In the case of SOS, the PEO block crystallizes and the fiber contracts inwards because of the resulting increase in density of these regions of the fiber. Analysis on this phenomena was accomplished by first performing a standard mechanical analysis until the fiber was at 5x its original length. Then, the instrument held the fiber at a constant length starting at the 1.5 second mark seen in Figure 10. The plot in

Figure 10 shows load versus time with a moving average of 15 periods. After about five seconds, an appreciable force was measured by the instrument as the fiber began to turn white which is an indicator of crystallization. This force was generated by the fiber contracting inwards because of the change in density between the original swollen amorphous phase of the hydrogel fiber and the dried semicrystalline phase of the PEO midblock.

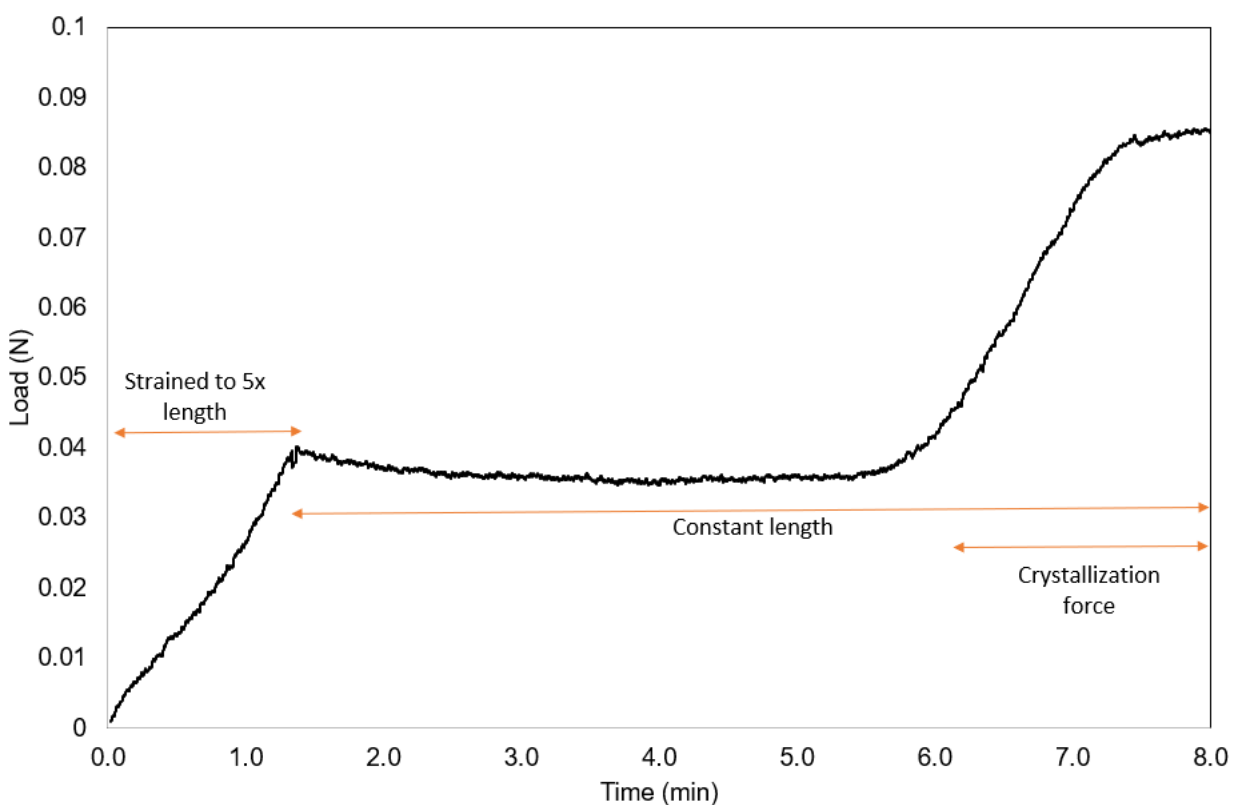


Figure 10: Load versus time plot for mechanical analysis of crystallization force

Chapter 3

Fiber Actuation Characterization Methods

3.1 Actuation Stroke

Actuation properties were evaluated by first straining the SOS hydrogel fibers produced via wet-spinning. The hydrogel fibers were strained to 5x their original length at a uniform strain rate on an MTS Exceed Model E 43 load frame, then left to dry and crystallize. Once the fiber was dried and appeared white it was removed from the load frame to air dry overnight. The dried, strained, SOS copolymer fibers were then ready to be actuated with heat or water. Heat actuation was triggered with a flat iron at 60 °C and water actuation was triggered by submerging the fiber in RO water. The actuation stroke measurement is thus a calculation of length change after actuation, and the equation used for this is seen by Equation 3.1. The theoretical full recovery actuation stroke is also calculated using Equation 3.1 and was used to compare to experimental values.

$$\text{Actuation Stroke} = \frac{\text{Strained length} - \text{Contracted length}}{\text{Strained length}} \quad (3.1)$$

To measure the reversibility of actuation properties, the actuation stroke was measured for two cycles. For the first cycle, the as prepared hydrogel fibers were strained to 5x their original length, left overnight to dry, and actuated with water. This process was repeated on the same fibers to investigate the influence of actuation cycle. A diagram of this process can be seen in Figure 11. Cycle dependence was evaluated for the actuation stroke, actuation speed, and energy density.

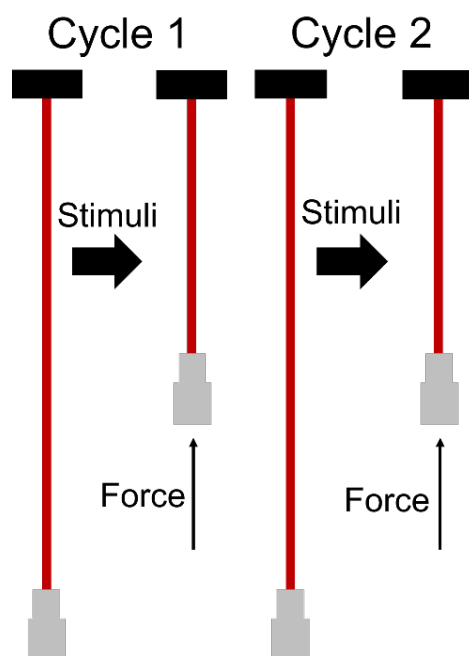


Figure 11: Diagram of method used to measure reversibility of properties

3.2 Actuation Velocity

The actuation velocity measured the speed at which the fibers actuate when triggered with heat or water for use as linear or rotary actuators. This was done by video analysis software and MATLAB code. For linear actuation, a 5x strained fiber was attached to a fixed clamp with a weight hanging at the bottom of the fiber. The mass of the weight and the diameter of the fiber were measured prior to the experiment. Then, for heat triggered actuation, a flat iron set to 60 °C was held beside the fiber to melt the PEO crystals and cause the fiber to actuate upwards. For water triggered actuation, a graduated cylinder filled with RO water was risen up to submerge the weight and the fiber which melts the crystals and also causes contraction of the fiber. The linear velocity was measured using software available from inLabPro.com to create a graph of strain/s and cm/s vs time which used Equation 3.2. The software allowed for the manual

selection of the fiber's position during each frame. This data could then be processed using Microsoft Excel to analyze the percent contraction over time caused by either water or heat given the initial length of the fiber.

$$\% \text{ contraction} = \frac{\text{Initial length} - \text{Contracted length}}{\text{Initial length}} \quad (3.2)$$

Rotational actuation analysis was performed by first rotating the hydrogel fiber prior to crystallization, and then holding it in place to allow it to dry. Through the use of SEM imaging, it was determined that the fibers were rotated to 7000 turns per meter [10]. Then, the fiber was attached to a fixed clamp with a vertically flat weight on the bottom that had a different color on each side. Then, similar to linear actuation, a flat iron was placed next to the fiber to heat it and the fiber spun with the weight attached. The rotational speed in rotations per minute (RPM) was measured using a MATLAB script which utilized the MATLAB computer vision toolbox. The MATLAB script was able to detect the color change, in terms of HSV color indices, of either side of the weight as a 0 or 1. This allowed for facile calculation of the rotations per frame based on the number of times the output changed from a 0 to a 1. The code was provided by MathWorks and was edited to adjust to the specific system and videos for analysis. The results were exported to Excel to calculate the rotations per minute achieved by the rotational actuation.

3.3 Energy/Work Density

The actuation experiments outlined in Chapter 3.2 can also be utilized to calculate the energy density of the SOS triblock copolymer fibers. Energy density, also known as work density, is a measure of work done normalized by the volume of the object doing the work. This is an important performance metric when comparing soft actuators because an advantage of

using polymers is their light weight. The mechanical properties of polymer fibers are able to rival that of other materials when the results are normalized by mass. Figure 12 shows an example of the length change seen with actuation. The equation which can be used to calculate the work performed by the fiber lifting a weight is $W = mg\Delta L$, where m is the mass of the weight being lifted, g is acceleration due to gravity, and ΔL is the distance the weight traveled upwards. Once the work has been calculated, this can be divided by the initial volume of the dried 5x strained fiber. The diameter of the fiber was measured through optical microscopy to evaluate the volume. Knowing these parameters, Equation 3.3 was used to calculate the energy density for each fiber.

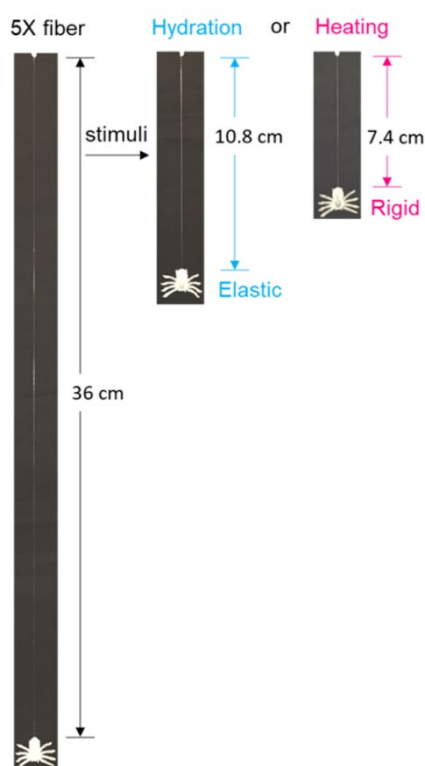


Figure 12: Example of actuation length change seen when fibers are exposed to water or heat [10]

$$\text{Work Density} = \frac{W}{V} = \frac{mg\Delta L}{\text{fiber volume}} \quad (3.3)$$

Chapter 4

Fiber Actuation Results and Discussion

4.1 Actuation Stroke

Actuation stroke was measured for several samples to evaluate the properties with respect to strain rate and cycle. First, actuation stroke was measured for two strain rates while initially straining SOS CE7 hydrogel fibers to 5x original length. As seen in Figure 13(a), the actuation stroke value did not change significantly between the two strain rates. The initial length of the fibers was 4 cm; therefore, the strain rates were 1 length per minute and 2 lengths per minute respectively. Figure 13(b) describes the minor difference in actuation stroke between two cycles of actuation for SOS CE3 fibers. This means that the fibers were strained and actuated with water two times to demonstrate the reversibility of actuation properties. The actuation stroke does not reach the fully recovered value of 0.8, but the fiber is able to successfully actuate and return to the same length for two cycles.

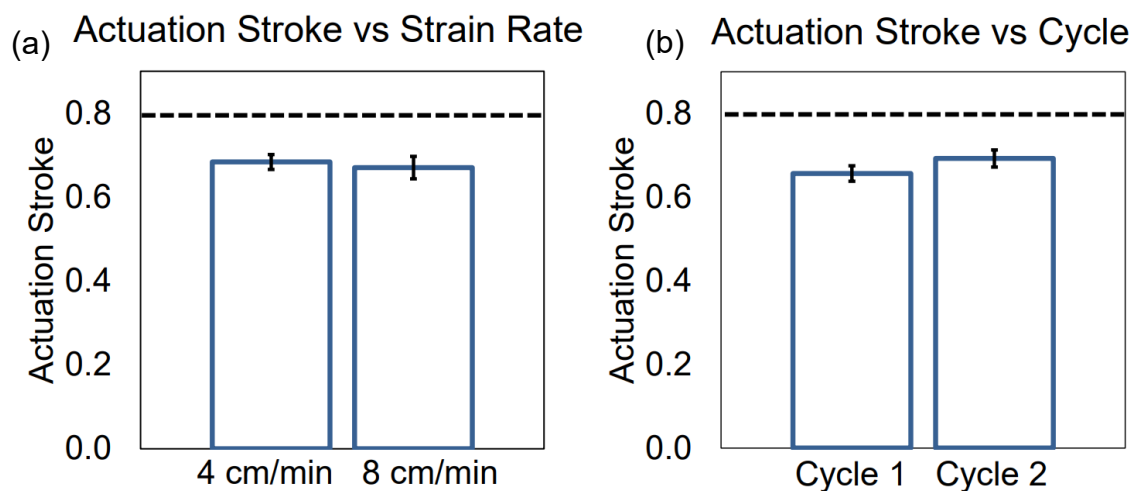


Figure 13: Plots of calculated actuation stroke values versus (a) change in initial strain rate and (b) number of times the fiber has been actuated

4.2 Actuation Velocity

Linear actuation results were calculated for three cycles of water triggered actuation of a weight at the end of an SOS CE3 5x strained fiber. The results in Figure 14(a) demonstrate the difference in velocity between cycles, but also shows that the fibers are capable of reversible linear actuation. Figure 14(b) includes a picture of the process of submerging the fiber into water to trigger actuation. The maximum linear actuation velocity and timescale of actuation achieved for each cycle are very similar. Cycle 3 does show a decrease in the amount of time required for fiber actuation compared to cycle 1 and 2, but more studies are necessary to predict the timescale property differences of linear actuation. The experiment involves submerging the fiber in RO water, and this may result in error from the drag force of the fiber and weight. Overall, these results show that linear actuation velocity results are reversible and the actuation properties are recoverable once the fiber is restrained.

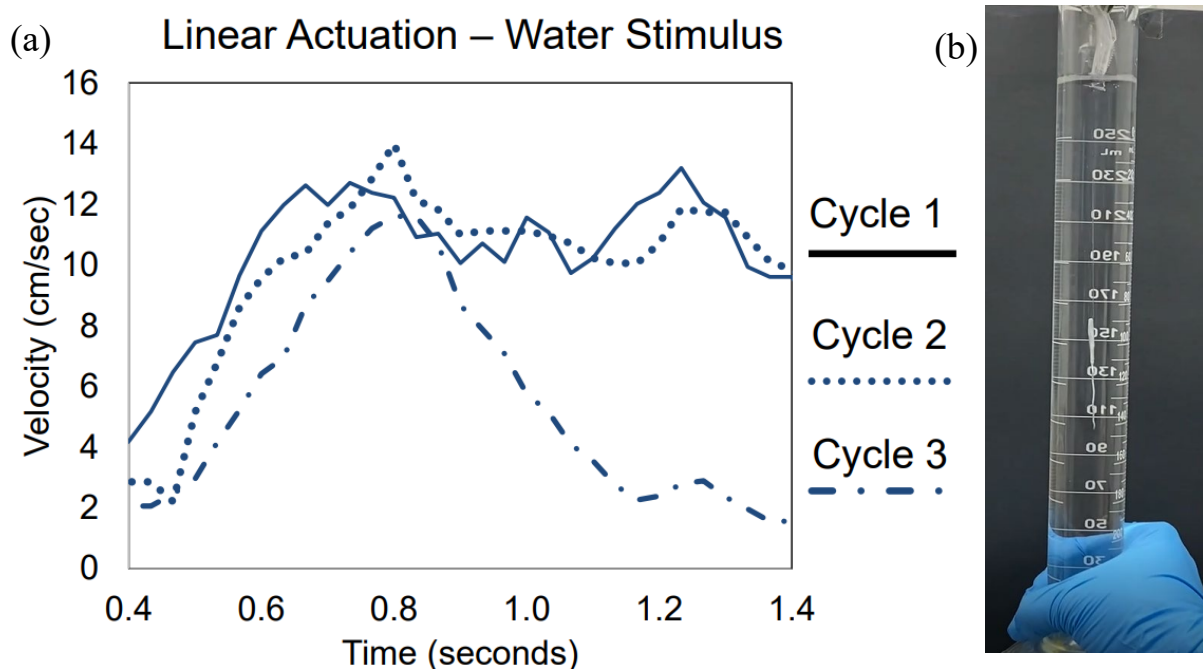


Figure 14: Plot of linear actuation speed versus the number of times the fiber has been actuated, and (b) picture of method of actuating fiber with water

Rotational actuation results were calculated for one cycle of water vapor triggered actuation for SOS CE3 fibers rotated to 7000 turns per meter. The rotational velocity results, measured in units of rotations per minute, are seen in Figure 15. A maximum velocity of around 400 rpm was calculated for the experiment, and it maintained a rotational speed of above 300 rpm for upwards of 10-15 seconds once actuated with water vapor. The results demonstrate the capabilities of a multifaceted actuator which can be stimulated by water to trigger controllable rotational force.

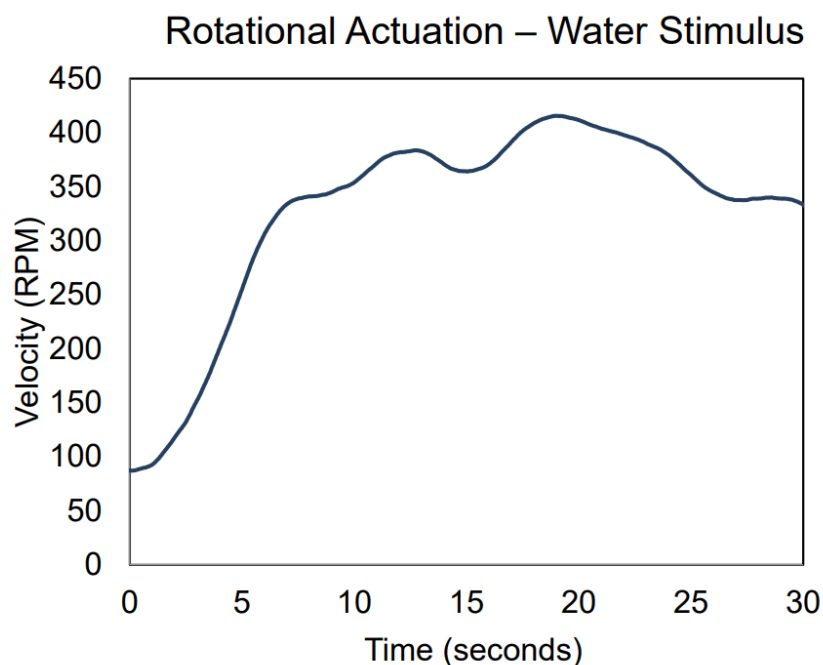


Figure 15: Plot of rotational actuation achieved for pre-rotated hydrogel fiber actuated with water

4.3 Energy/Work Density

An important indicator of actuator performance is the energy density. The energy density is highly dependent on the volume of the fiber and therefore dependent on the diameter of the fiber and needle gauge size used during wet-spinning. For the data in Figure 16(a), fibers made

from SOS CE3 were actuated for two cycles, and the results showed that the energy density is a reversible property which is important for potential use in soft actuator applications. Energy density values are larger for the second cycle because the diameter of restrained fibers was smaller than the fiber from the first cycle. It is hypothesized that since the fiber does not fully recover its original length after the first cycle, then when it is strained to 5x again it will have a smaller diameter and volume.

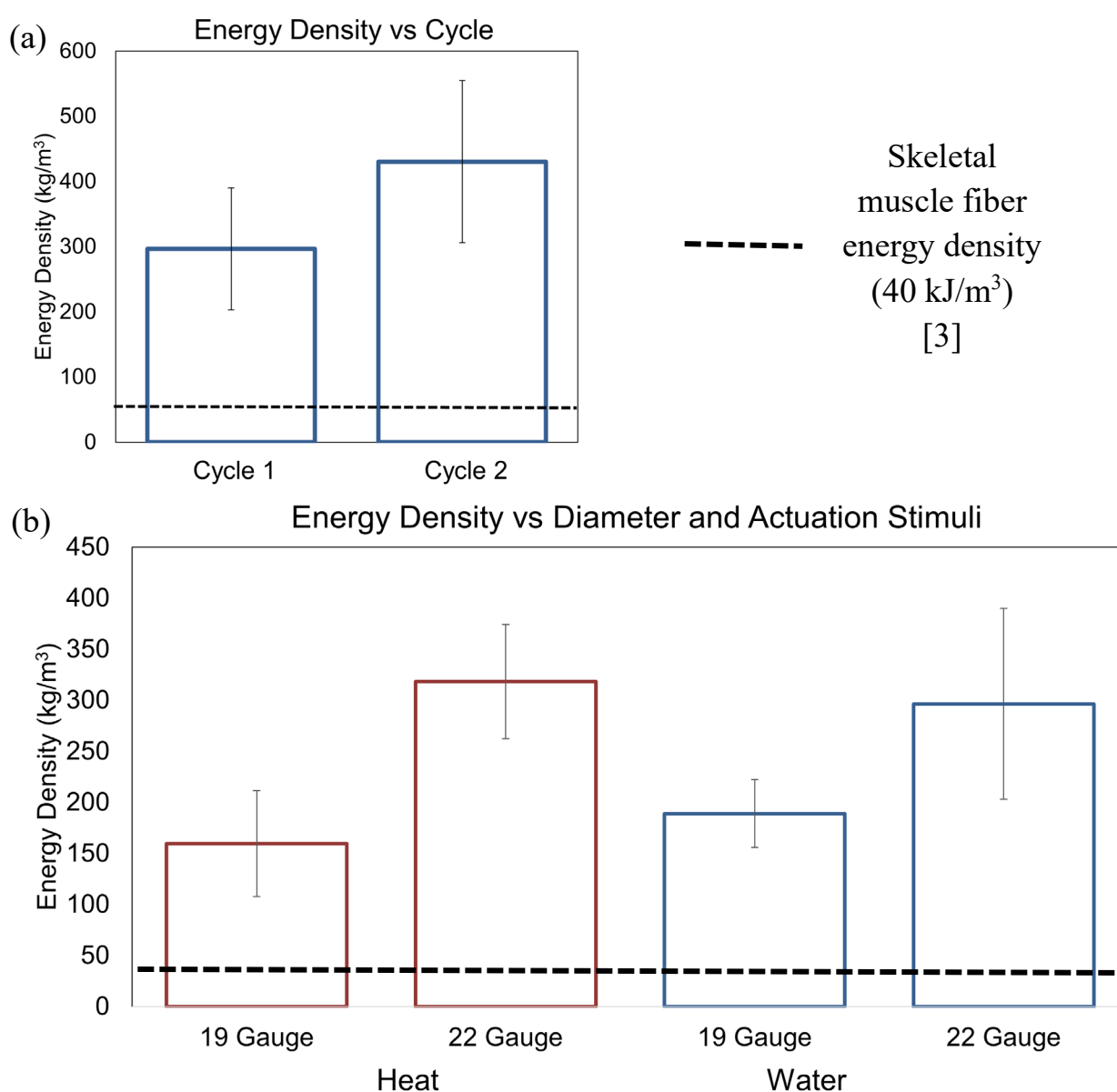


Figure 16: Energy density versus (a) cycle, (b) actuation trigger, and needle gauge

The energy density results for different needle gauges and actuation triggers for fibers made from SOS CE3 are shown in Figure 16(b). The 19 gauge, which is a larger nozzle diameter, has a lower energy density for both actuation triggers because of its larger diameter and thus larger volume of fiber used. Since energy density is highly dependent on the volume of the actuator, this had a large effect on the calculations. When comparing the energy density between fibers actuated with water or heat, there is not an appreciable difference, and they are within one standard deviation of one another. The energy density values for each experiment exceeded the maximum literature value for skeletal muscle fiber energy density [3].

Chapter 5

Conclusion and Future Work

In summary, the triblock copolymer system of polystyrene-*b*-poly(ethylene oxide)-*b*-polystyrene was evaluated for potential use in applications of soft robotics and artificial muscles. Fibers produced via wet-spinning were strained to 5x their original swollen length which causes the PEO blocks to crystallize along the fiber direction. The force generated during polymer crystallization was measured by mechanical analysis of a fiber held at 5x strain to induce crystallization. To evaluate actuation properties, the strained fibers were actuated by the presence of water or heat. Actuation triggered a response which caused the fibers to shorten towards their original length as described by the actuation stroke, and a contraction force was measured and characterized by the actuation velocity and energy density. The actuation stroke, actuation velocity, and energy density were all recoverable properties as shown through the reversibility of results for each value for a second cycle of actuation. Property recovery is critical for potential uses in soft actuators. The resulting energy density values were also significant because the values for each cycle and needle gauge diameter were greater than the literature value recorded for skeletal muscle fibers.

Future work for this project includes further research into the effects of cycle lifetime on actuation properties past two cycles. Hysteresis in mechanical properties is an important consideration for the lifetime of actuators in real-world applications and should be studied in greater detail for this dynamic fiber system for both heat and water triggers. Also, there is the potential for more work to be done regarding understanding the structure-processing-property relationships between wet-spinning and fiber properties. For example, further experiments could be done to study the effects of injection speed and water bath temperature. Once these

relationships are defined, it will allow for a facile transition to large scale wet-spinning to create large quantities of fibers in a process similar to industrial applications. Further work can also be done to understand how weaving the fibers can lead to unique properties in the field of textile actuators. Finally, there is potential for this system to be replicated for other ABA triblock copolymer systems to explore further properties and applications. For example, future research may include preparation of poly(lactic acid)-*b*-poly(ethylene oxide)-*b*-poly(lactic acid) for bioresorbable uses and drug delivery in the medical field. Overall, this thesis project provides a framework and preliminary results to study how triblock copolymers can be utilized to further the field of soft robotics and artificial muscles.

BIBLIOGRAPHY

1. Rothmund, P., Kim, Y., Heisser, R. H., Zhao, X., Shepherd, R., F., & Keplinger, C. (2021). Shaping the future of robotics through materials innovation. *Nature Materials*, **20**, 1582-1587
2. Hines, L., Petersen, K., Zhan, G., & Sitti, M. (2017). Soft Actuators for Small-Scale Robotics. *Advanced Materials*, **29**, 1-43
3. Li, M., Pal, A., Aghakhani, A., Pena-Francesch, A., & Sitti, M. (2022). Soft actuators for real-world applications *Nature Review Materials*, **7**, 235-249
4. Cianchetti, M., Laschi, C., Menciassi, A., & Dario, P. (2018). Biomedical applications of soft robotics. *Nature Reviews Materials*, **3**(6), 143–153.
5. Acome, E., Mitchell, S. K., Morrissey, T. G., Emmett, M. B., Benjamin, C., King, M., Radakovitz, M., & Keplinger, C. (2018). Hydraulically amplified self-healing electrostatic actuators with muscle-like performance. *Science*, **359**, 61-65
6. Kanik, M., Orguc, S., Varnavides, G., Kim, J., Benavides, T., Gonzalez, D., Akintilo, T., Cem Tasan, C., Chandrakasan, A., Fink, Y., & Anikeeva, P. (2021) Strain-programmable fiber-based artificial muscle. *Science*, **6**, 57
7. Maziz, A., Concas, A., Khaldi, A., Stalhand, J., Persson, N., & Jager, E. W. H. (2017) Knitting and weaving artificial muscles. *Science Advances*, **3**(1)
8. Lang, C., Lanasa, J. A., Utomo, N., Xu, Y., Nelson, M. J., Song, W., Hickner, M. A., Colby, R. H., Kumar, M., & Hickey, R. J. (2019). Solvent-non-solvent rapid-injection for preparing nanostructured materials from micelles to hydrogels. *Nature Communications*, **10**(1).
9. Mirabedini, A. (2018) Introduction and Literature Review. Developing Novel Spinning Methods to Fabricate Continuous Multifunctional Fibres for Bioapplications. *Springer International Publishing*, pp. 1–45

10. Lang, C., Lloyd, E. C., Matuszewski, K. E., Xu, Y., Ganesan, V., Huang, R., Kumar, M., Hickey, R. J. (2022). Nanostructured Block Copolymer Muscles. *Nature Nanotechnology*, *Accepted*.
11. Wang, Y., Liu, C., Ren, L., & Ren, L. (2022). Bioinspired soft actuators with highly ordered skeletal muscle structures. *Bio-Design and Manufacturing*, **5**, 174-188.

ACADEMIC VITA
Kelly E. Matuszewski
kem6169@psu.edu

EDUCATION

Pennsylvania State University, University Park, PA Expected Graduation: May 2022
Schreyer Honors College
B.S. in Materials Science and Engineering, Minor in Polymer Science

RESEARCH EXPERIENCE

Penn State University, Department of Materials Science and Engineering

Undergraduate Researcher: Dr. Robert Hickey Research Group *September 2018-present*

Project 1 – Honors Senior Thesis August 2021-present

- Analyzing crystallization and reversible actuation for wet-spun polystyrene-b-polyethylene oxide-b-polystyrene (SOS) triblock copolymer fibers

Project 2 – Literature review and remote data analysis May 2020-August 2020

- Developed white paper for novel production method of SOS triblock copolymer hydrogel fibers via wet-spinning
- Created MATLAB code for remote visual data analysis of shape memory properties

Project 3 – Property analysis of triblock copolymer fibers October 2018-May 2021

- Studied shape memory, mechanical, and structure properties of SOS hydrogel fibers, shadowed anionic polymerization technique, and learned research techniques focused on self-assembly of nanostructured hydrogels
-

PUBLICATIONS

Lang, C., Lloyd, E., **Matuszewski, K.E.**, Xu, Y., Ganesan, V., Huang, R., Kumar, M., Hickey, R.J.
“Nanostructured Biomimetic Block Polymer Muscles” *Nature Nanotechnology*
In Revision.

WORK EXPERIENCE

Schrödinger Inc., Materials Science Intern *May 2021-August 2021*

- Analyzed properties found via molecular dynamic simulations of polymeric materials with varying molecular weight and dispersity while developing skills in computational methods
- Worked with collaborative team to help validate feature for polydispersity software release

Penn State University, College of Agricultural Sciences *September 2020-present*

Teaching Assistant: Agriculture/CED 160: Introduction to Ethics and Issues in Agriculture

- Facilitate discussions, create quizzes, grade weekly essays, and help manage course page and grades for class of over 70 students

Penn State University, Department of Chemistry *August 2019-December 2019*

Learning Assistant: Chem 202: Fundamentals of Organic Chemistry I

- Developed teaching skills by hosting weekly review sessions and attending classes to assist with problem sets and questions regarding class content
-

HONORS AND AWARDS

Dean's List: Penn State University *Fall 2018, Spring/Fall 2019, Spring/Fall 2020, Spring 2021*

- Achieved a GPA of 3.5 or higher for every semester

Laureate: Earth and Mineral Sciences Academy for Global Experience (EMSAGE) *October 2021*

- Demonstrated success in scholarship, experiential learning, global literacy, and service

Best in Junior Semester Standing: EMS Celebration of Undergraduate Engagement *March 2020*

- Matuszewski, K.E., Hickey, R.J., Lang, C. *Mechanical Properties of Hydrogel Fibers from Rapid Injection*. College of EMS Celebration of Undergraduate Engagement (CUE). March 2020.

Scientific Category Third Place: PSU Materials Visualization Competition *March 2020*

- Matuszewski, K.E., *Hydrogel Fiber After Resubmerged into Water*, Materials Visualization Competition. March 2020.

Undergraduate Research Fellow Recipient: PSU MatSE Department *October 2019-May 2020*

- Awarded grant to pursue research with Dr. Hickey's research group

President's Freshman Award: Penn State University *January 2019*

- Awarded to students who achieve a 4.0 during their first semester

LEADERSHIP/EXTRACURRICULARS

Women in the College of Earth and Mineral Sciences (WEMS), President *May 2021-present*

- Lead and coordinate a supportive club for undergraduate women in the College of Earth and Mineral Sciences focused on professional development events

U.P.U.A., Executive Director of Environmental Sustainability *January 2021-December 2021*

- Manage the Department of Environmental Sustainability within Penn State's student body government, leading a team of 8 directors working on sustainability projects at Penn State

College of EMS Ambassador *August 2020-present*

- Work to promote the College of EMS to prospective students through tours and panels

Outdoor Volleyball Club *August 2019-present*

- Participate in intramural tournaments and recreational volleyball with members

Earth and Mineral Sciences Student Council, EMEX Chairperson *September 2018-present*

- Coordinate team to plan and organize an informative event for prospective EMS students

SCHOLARSHIPS

Penn State Department of Materials Science and Engineering

- Vladimir Stubican Undergraduate Scholarship in MatSE *2021-2022*
- Sam Zerfoss Memorial Scholarship *2020-2021*
- Guy and Rae Rindone Award for Academic Excellence in MatSE *2020*
- Charles D. Greskovich Memorial Scholarship *2019-2020*
- Norris B. McFarlane Scholarship *2019*
- Anthony J. and Alberta L. Perotta Scholarship *2019*

Penn State College of Earth and Mineral Sciences

- Matthew J. Wilson Honors Scholarship *2018-2022*

Penn State University

- 4 Year Provost Award *2018-2022*